

Palladium and platinum complexes of folic acid as new drug delivery systems for treatment of breast cancer cells



Chenyang He^a, Mostafa Heidari Majd^{b,*}, Fereshteh Shiri^c, Somaye Shahraki^c

^a Department of Oncology, The Second Affiliated Hospital of Xi'an Jiaotong University, Xi'an, 710004, China

^b Department of Medicinal Chemistry, Faculty of Pharmacy, Zabol University of Medical, Sciences, Zabol, Iran

^c Department of Chemistry, University of Zabol, Zabol, Iran

ARTICLE INFO

Article history:

Received 10 November 2020

Revised 19 December 2020

Accepted 21 December 2020

Available online 24 December 2020

Keywords:

Metallo-complexes

Real-time PCR

Targeting drug delivery

Molecular docking

Bak1/Bclx ratios

ABSTRACT

Cisplatin is administrated as an agent in treatment of various cancers by intercalation between DNA strands and inhibition of DNA replication. Among the various factors, two important reasons like inhibition of apoptosis by anti-apoptotic mechanisms and inability to distinguish normal cells from cancerous led us to synthesize two new complexes of platinum and palladium containing folic acid (FA). Following, the cytotoxic effects of complexes were studied using MTT assay in MCF-7 cells, then expression levels of Bak1, Bclx and Caspase-3 genes were elucidated by Real-time RT-PCR technique. Also, the behavior of complexes in the binding sites of folate receptor was described by molecular docking. All experiments have confirmed that presence of FA could improve cytotoxicity, apoptosis and cellular uptake of cisplatin in MCF-7 breast cancer cells. In addition, formation of 2,2'-bipyridine palladium(II) chelate with FA decreased the anti-apoptotic Bclx levels in comparison with cisplatin.

© 2020 Elsevier B.V. All rights reserved.

1. Introduction

One of the most important of transition metal complexes is cisplatin and its analogs (carboplatin, oxaliplatin) which are used in treatment of various cancers such as ovarian, colorectal, breast, stomach and prostate [1]. This yellow crystalline powder is slightly soluble in water and may transform slowly over time to the trans-isomer [2]. Cisplatin has a square planar geometry because of the four d_{sp^2} hybrid orbitals, so it can intercalate between DNA strands and inhibit its replication. According to this mechanism, it is probably that cisplatin does not distinguish the difference between normal cells and cancerous cells, and causing inadvertent severe side effects [3, 4]. On the other hand, the treatment of multiple cancers with cisplatin is accompanied by drug-resistant, because they can change the cellular uptake, inhibit the apoptosis by anti-apoptotic mechanisms and also increase the detoxification, drug efflux and DNA repair [4]. To overcome cisplatin resistance and side effects, over 1000 complexes of platinum (Pt), platinum-group metals such as palladium (Pd), transition metals and also other rare earth metals were synthesized during the last decades [5-7]. Also, various ligands with crucial biological activities were considered to developing the metal complexes.

Amongst these ligands, bipyridine (bpy) has gained popularity because of their π stacking interactions with DNA base pairs through van der waals forces and also hydrophobic forces. Moreover, the two nitrogen atoms in the heterocyclic rings allow them to maximize their potential and acting as versatile chelating agents. Several studies have shown that these nitrogen-chelating compounds show individual anticancer activities through interactions with cancer-related receptors, on the other hand, they can bind to human serum albumin (HSA) which plays a significant role in delivery of metal-based complexes to their cellular targets. In general, it is confirmed that bipyridine can coordinate with palladium to form strong enough and soluble complexes in aqueous media [8]. For instance, Asensio and co-workers [9] and Didgikar et al. [10] have synthesized and characterized water-soluble palladium complexes with bpy, and have studied their application as anticancer agent against cancer cells.

Although, only 40 agents from over 600,000 compounds in testing phase were used in clinical stage; because many of them haven't specific effects on target tumor cells and their usage have been limited as drugs for malignancies [11]. Furthermore, current platinum drugs and analogues cannot target a specific receptor and this poorly differentiating between cancer and normal cells is still a major drawback of them. The active delivery of metal-based complex drugs toward special receptors may significantly improve drug penetration into tumors, as well as reducing the off-target side effects of the chemotherapeutic drugs. Active targeting can be per-

* Corresponding author.

E-mail address: mostafamajd@live.com (M. Heidari Majd).

formed by conjugation of a receptor mediated endocytosis agent to recognize the specific high-expressed receptors and also reduce the incidence of side effects.

In our previous works, we had used of folic acid (FA) as a targeting moiety for the folate receptors (FRs) that are often highly expressed on the surface of breast cancer cells [12, 13]. Addition to its biological functions, formation of cisplatin chelates with FA may be led to extended release half-life, long blood circulation time plus specific and efficient cellular uptake. To test all possibilities, we began by formation of eight-membered rings of 2,2'-bipyridine palladium(II) and also cisplatin via folic acid, then evaluated the cytotoxicity of them on MCF-7.

2. Materials and method

All chemicals were purchased from Sigma-Aldrich (St. Louis, MO, USA). MCF-7 cell line was obtained from Pasture Institute (Tehran, Iran). All media and cell culture components were obtained from either Caisson labs (North Logan, UT) or Gibco (Carlsbad, CA). High Pure RNA Isolation Kit was obtained from Roche (Rotkreuz, Switzerland). EasyTM cDNA Synthesis kit was purchased from Pars Tous Biotechnology (Mashhad, Iran).

2.1. Synthesis of 2,2'-bipyridine palladium(II) dichloride complex [Pd(bpy)Cl₂]

As described in previous works [14], PdCl₂ (0.885 g, 5.0 mmol) and NaCl (2.922 g, 50 mmol) was dissolved in a 100 ml flask containing 50 ml distilled water and was stirred for 30 min at 60 °C. 2,2'-bipyridine (0.780 g, 5.0 mmol) was dissolved in 100 ml of water-ethanol (1:1 v/v) and then was added dropwise to the above solution while stirring vigorously with the aid of the magnetic stirrer. Stirring continued for another 2 h at RT and the crude yellowish precipitate was filtered and then washed several times with water, ethyl alcohol and acetone, respectively. Finally, the products were dried at 40 °C. Yield was 93%.

2.2. Replacement of chloride ligands by aqua groups

Converting of [Pd(bpy)Cl₂] to [Pd(bpy)(H₂O)₂](NO₃)₂ was done as described previously works [15]. For this purpose, [Pd(bpy)Cl₂] (9 mg, 0.027 mmol) was suspended in 15 mL of buffer solution of acetic acid and sodium acetate with pH of 3.5. Then, 9.17 mg of AgNO₃ (0.054 mmol) was added to the reaction mixture while stirring was done in darkness for 7 h at 60 °C and then 12 h at RT (30 °C). Whereupon the precipitated AgCl immediately removed by centrifugation. Also, this process was done entirely for cisplatin (10 mg, 0.033 mmol) utilizing 11.21 mg of AgNO₃ (0.066 mmol) to form the diaqua species of it, cis-[Pt(NH₃)₂(H₂O)₂](NO₃)₂.

2.3. Synthesis of metal complexes of folic acid

For the first step, the pH of the folic acid solution is adjusted to about 7.6–7.8 by adding 2.2 equivalent excess of NaHCO₃ at about ~60 °C with 125 rpm shaking for 10 min. Synthesis of two complexes were done in two separate flasks. i, [Pd(bpy)(H₂O)₂] complex was stirred in 70 °C for 30 min and then the FA solution (11.92 mg, 0.027 mmol) was added dropwise to the reaction mixture over 1 h and was stirred for another 6 h at 50 °C. ii, cis-[Pt(NH₃)₂(H₂O)₂] complex was stirred in 70 °C for 30 min and then the FA solution (14.57 mg, 0.033 mmol) was added dropwise to the reaction mixture over 1 h and was stirred for another 6 h at 50 °C. The products were vacuum rotary evaporated to dryness (60 °C, 250 rpm). The metal folate complexes were dispersed in 10 ml acetonitrile/methanol (1:1) and then separated out from its solution

by filtration and washed with acetone and kept in a vacuum desiccator over dried silica gel. The steps of synthesis were validated by FTIR spectroscopy using Shimadzu IR PRESTIGE 21 spectrophotometer (Shimadzu Scientific Instruments, Tokyo, Japan). Also NMR analysis of final complexes was taken up in D₂O by a BRUKER 500 MHz AVANCE III (Bruker, Rheinstetten, Germany) instrument.

2.4. Cell culture and in vitro cytotoxicity testing: MTT assay

Human breast cancer MCF-7 cells were routinely grown in 25 cm² culture flasks at a seeding density of 5.0 × 10⁴ cells/cm² using RPMI 1640 media supplemented with 10% FBS plus 100 μL of Penicillin G/Streptomycin [16, 17]. A CO₂ incubator was used to culture cells according to existing standards during cultivation and during experiments. When MCF-7 cell lines reach about 80% confluence, the cells at a density of 1.2 × 10⁴ cells/well were transferred onto 96-well culture plates and incubated for 24 h. Thereupon, the cells were treated with [Pd(bpy)FA], cis-[Pt(NH₃)₂FA] and cisplatin at eight different concentrations (ranging from 6.25 to 800 μM) for two period of 48 and 72 h. In timely manner, the media was removed and cells were subjected to 200 μL of MTT solutions composed of 150 μL of fresh media plus 50 μL of MTT solutions (prepared as 2 mg/mL in PBS). Thereafter, plates were incubated for 4 h at 37 °C in a CO₂ incubator. Finally, the media was aspirated off and absorbance of formed formazan crystals was recorded at 570 nm utilizing a spectrophotometer (BioTek Instruments, Inc., Bad Friedrichshall, Germany) and by adding 200 μL of DMSO.

2.5. Real-time PCR analysis

For an incubation period of 24 h, MCF-7 cells (acceptable range: 1.0 × 10⁶ in T-25 culture flask) were treated with 50, 100 and 300 μM of cisplatin, cis-[Pt(NH₃)₂FA] and [Pd(bpy)FA], respectively [18]. One flask without any treatment was also prepared as control. After which the cells were washed with PBS and were dissociated from adherent surface using trypsin, they were centrifuged at 3000 rpm for 5 min and resuspended in 200 μL PBS. Isolation of total RNA from cultured cells was performed using High Pure RNA Isolation Kit according to the manufacturer's protocol. Briefly, cells were lysed using 400 μL Lysis/-Binding buffer and were adjacent to 90 μL DNase Incubation buffer plus 10 μL DNase I to remove genomic DNA contamination. Total isolated RNA was collected by adding of 100 μL Elution buffer into a clean, sterile 1.5 mL microcentrifuge tube. Purity and concentration of the isolated RNA were determined by WPA Biowave II spectrophotometer (Biochrom Ltd, Cambridge, UK) which absorbs over the 230–260 nm range. They were stored at –80 °C for later analysis.

Complementary DNA (cDNA) was synthesized using Pars Tous EasyTM cDNA Synthesis kit according to the manufacturer's protocol. Accordingly, four separate mixtures of 10 μL 2X buffer mix, 2 μL enzyme mix, 6 μL isolated RNA and 2 μL DEPC-treated water were prepared for total volume of 20 μL. Then, the reaction mixtures were incubated at 25 °C for 10 min, 47 °C for 60 min and 85 °C for 5 min. Relative quantitation with RT-PCR was done for apoptotic genes GAPDH- TTGCCATCAATGACCCCTTCA, CGCCCCACTTGATTTTGGGA, Bak1-TCTGGGACCTCCTTAGCCCT, AATGGGCTCTCACAAGGGTATT, Bclx-TGGAAAGCGTAGACAAGGAGA, TGCTGCATTGTTCCCATAGA and Caspase-3- TGCAGTCATTATGAGAGCAAT, AAGGTTTGAGCCTTTGACCA using Applied Biosystems StepOneTM instrument (Thermo Fisher Scientific, Massachusetts, USA) through the following thermal cycling conditions: an holding stage at 95 °C for 12 min followed by 40 cycles of 95 °C for 20 s, 55 °C for 20 s and 72 °C for 20 s, and finally melt curve stage at 95 °C for 15 s, 60 °C for 60 s and 95 °C for 15 s. All reactions were independently performed in duplicate, and the average cycle

threshold (CT) value was used for analysis. The GAPDH was used as housekeeping gene for the normalization of CT values and the fold change expression was calculated by $\Delta\Delta\text{CT}$ method [19].

2.6. Molecular dynamic simulation

The molecular dynamics simulation technique was performed in order to provide a more refined and flexible structure systems model for the docking procedure [20]. The crystal structures of folate receptor (FR) was downloaded from the Protein Data Bank (PDB), along with the ID numbers of 4LRH [21]. Preparation the protein including added hydrogens and missing atoms were done using the web application playmolecule (www.playmolecule.org) [22]. Then, the water molecules removed. MD simulation was done using the Gromacs 2019 simulation package running on a GPU server. Amber99sb force field at a mean temperature of 300 K and the physiological pH of 7 was applied. Chimera software [23] calculated the AM1 partial charges and acpype program [24] generated the topology and coordinate files for the docked inhibitor. A solute box distance of 1.0 nm was specified which sets the minimum distance of 2.0 nm between any two periodic images of a protein complex. The box was filled with TIP3P water molecules and the system was neutralized with the addition of Na^+ ions. Optimization of the system was applied using the steepest descent algorithm through a 100 ps run. Then, during the first equilibrium step, atom positions of the macromolecule and ligand were targeted to a position restraint using a force constant of $1000 \text{ kJ mol}^{-1} \text{ nm}^{-2}$ in an NVT ensemble for 500 ns and the temperature was regulated to 300 K via V-rescale thermostats. Afterward, the pressure of the system was stabilized under the NPT ensemble over the course of the 500 ps equilibration phases. Finally, a 100 ns production MD simulation was run for data collection under a well equilibrated system with a desired temperature and pressure. The long-ranged electrostatic contributions were treated using the particle-mesh Ewald (PME) method. The LINCS constraint algorithm was used to constrain lengths of all covalent bonds. Finally, the protein was returned to the box center and the trajectory was corrected in terms of the periodic boundary condition. The root-mean-square deviation (RMSD) was calculated for the protein backbone atoms of each frame over the entire course of the MD simulation against the first frame as the reference to further define the equilibrium time range.

2.7. Molecular docking

The binding pose, key interactions and the binding affinity of the protein-ligand complex were anticipated using molecular docking [25, 26]. The mol structures of two complexes were generated by Chem3D 15.0 and converted into single SDF chemical table format using Open Babel (v2.3.0). Since the X-ray crystallography of the complex structures is not available, for this purpose we used the DFT model described in the methodology section. The structures were optimized by Gaussian 09 at Density Functional Theory (DFT) procedure in B3LYP level with a LanL2DZ basis set for Pd and Pt and 6-31 G basis set for other atoms. The LANL2DZ basis set contains diffuse and polarization functions, as well as effective core potential [27]. The output trajectories of MD simulation was using to molecular docking simulation. An evaluated flexible molecular docking was performed using GOLD [28] using ChemScore fitness function. The Genetic algorithm (GA) is used in GOLD ligand docking to examine the ligand conformational flexibility, along with the partial flexibility of the protein. The maximum number of runs was set to 10 for each complex, with the default parameters (100 population size, 5 for the number of islands, 100,000 number of operations and 2 for the niche size). Default cut off values of 2.5 \AA (dH-X) for hydrogen bonds and 4.0 \AA for van-der-Waals distance were used. When the solutions attained RMSD values within 2 \AA , GA docking was terminated. According to the subsequent docking results, the lowest energy docked conformation, was selected as the binding mode. The visualization of the docking results was conducted by applying BIOVIA Discovery Studio client 2016. The interacting energies between each amino acid with the lowest docking energy of the complexes into binding site of protein, separately were calculated by Molegro Molecular Viewer 2.5 (MMV) (<http://www.molegro.com/mmv-product.php>).

3. Result and discussion

3.1. Infrared spectra of metal complexes

In this study, prepared complex between folic acid and cis-platin, as well as complex formed between folic acid and palladium(II) were confirmed using FTIR. This method is an appropriate technique to understand the intermolecular interaction of complexes and a comparison of FTIR spectra of folic acid with that of

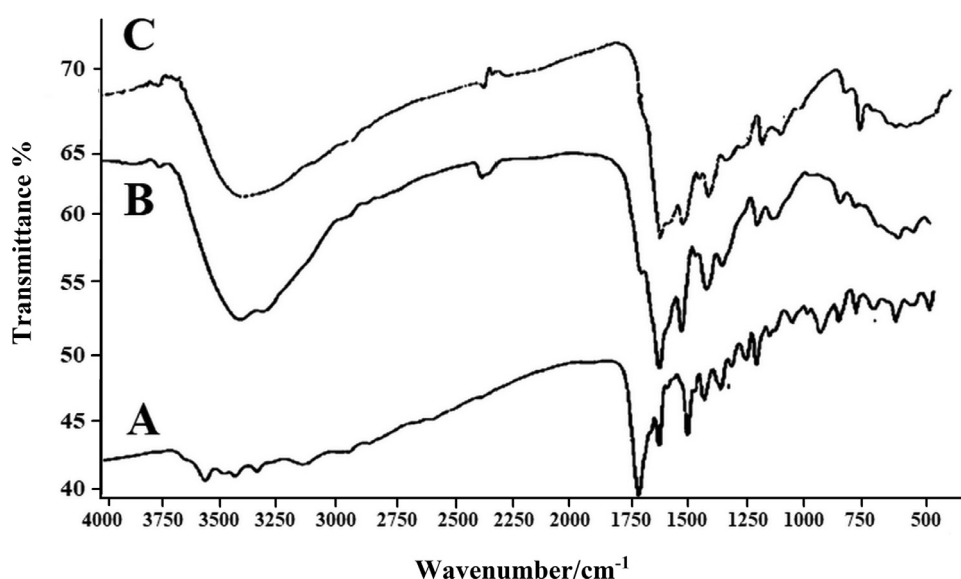


Fig. 1. FTIR spectra of A) pure Folic acid, B) cis-[Pt(NH₃)₂FA] and C) [Pd(bpy)FA].

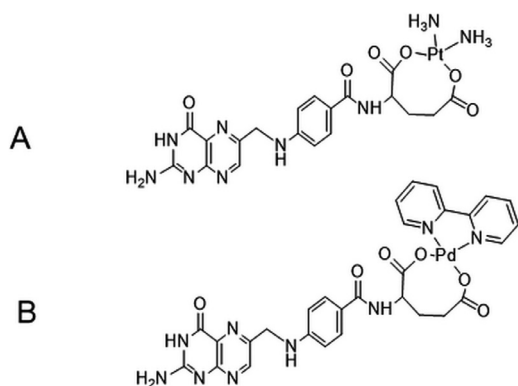


Fig. 2. Structures of newly synthesized complexes. A) *cis*-[Pt(NH₃)₂FA] and B) [Pd(bpy)FA].

the products after interaction. As shown in Fig. 1A, the bands for pure FA between 3300–3550 cm⁻¹ are due to the hydroxyl (OH) and NH groups of glutamic acid moiety and of pterin ring, respectively. Also, the stretching vibration peak related to C=O of carboxyl groups appears at 1701cm⁻¹, while the bending mode of NH groups are clear at 1604cm⁻¹. One highlight of the pure FA spectrum is that there is no absorption peak between 2000 and 2800cm⁻¹ [29].

When folic acid formed a complex with Pt or Pd, small shifts in the absorption peaks position with respect to pure FA occur, as obvious in Fig. 1B and C. Furthermore, a new band appears at ~2300cm⁻¹ which is ascribed to C=N+H of pterin ring [30], while the stretching vibration of C=O (1701cm⁻¹) of free carboxylic groups is shifted or disappeared in the spectra of prepared complexes which is depended on the coordination mode of the COO⁻ group with the metal ions [31]. This fact revealed that both carboxyl groups would change by the same amount and participate as monodentate ligand, therefore the expected structures of the two complexes are according to Fig. 2 [32]. In other words, FA generally acts as a bidentate ligand via two monodentate carboxylate groups [31].

If pay special attention to FTIR spectrum of *cis*-[Pt(NH₃)₂FA] (Fig. 1B), two strong peaks are seen at 3294 and 3394 cm⁻¹ which ascribed to primary amines of cisplatin [33], while Fig. 1C showed an absorbance in 3410 cm⁻¹ related to secondary amine groups of FA.

DFT calculations can provide molecular-level information that used to valid the experimental IR spectra. As can be seen in Fig. 3 our DFT/B3LYP calculations show that the experimental and quantum chemical calculations are consistent.

From the ¹H NMR results, it is conceivable that two complexes are formed. The specific frequencies related to *cis*-[Pt(NH₃)₂FA] showed clearly chemical groups attributable to FA moiety: (δ 1.98–2.28 related to 4H of methylene groups, -CH₂-CH₂-), (δ 4.39 related to 2H of another methylene, Ph-NH-CH₂-), (δ 4.42 related to 1H of methine, -CO-NH-CH-CO-), (δ 6.71–7.2 related to 4H of phenyl group), (δ 8.34 related to 1H of amide group, Ph-CO-NH-), (δ 8.61 related to 2H of amine group of pteridine ring) and (δ 9.03 related to 1H of 2-pyrazine ring).

In ¹H NMR spectrum of [Pd(bpy)FA], in addition to the specific frequencies of FA, peaks related to 8H of -CH- groups attributable to bpy are also detected at δ 7.09, 7.57, 8.59, and 8.78.

3.2. Cytotoxicity effects of metal complexes

Due to the efficacy of DNA crosslinkers in broad number of malignancies, almost half of patients with cancer receive cisplatin or its analogues as standard chemotherapeutic regimens [34]. Unfor-

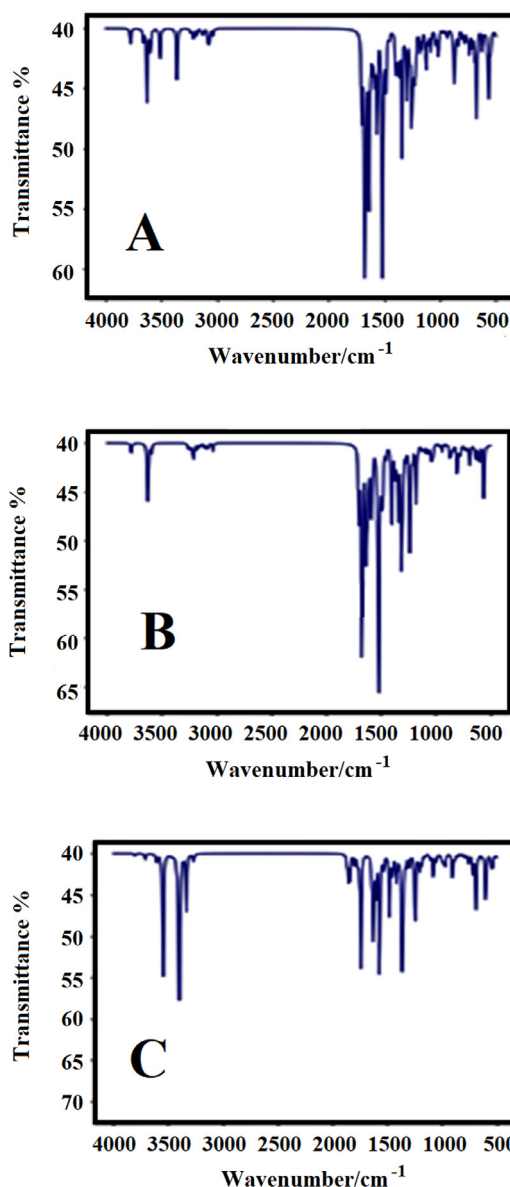


Fig. 3. The theoretical IR spectra for (a) complex A (b) complex B (c) Folic acid.

tunately, cytotoxicity or apoptosis are sometimes induced in normal cells, thus, platinum complexes might also lead to diverse side-effects such as bone marrow-suppression, peripheral neuro-renal-toxicity [35]. Hence, there is particular interest in the synthesis of the anticancer agents with new metals and ligands to minimize severe side effects. One of the best metals with similar hypoallergenic properties with platinum is palladium, and one of the best DNA intercalator ligands is bipyridine. Many works confirmed that Pd complexes containing bpy are highly effective against several cancer cell lines [36–38], but in none of them the targeted delivery into tumor cells weren't anticipated.

Therefore, we decided to synthesis two new complexes of Pt and Pd utilizing folic acid with the aim of prolong drug action and maintenance of prescribed dose within a therapeutic window. Since the FRs are overexpressed on MCF-7 cell lines [12], they were selected for cytotoxicity evaluation of *cis*-[Pt(NH₃)₂FA] and [Pd(bpy)FA] in comparison to cisplatin. As it is illustrated in Fig. 4, the viability of MCF-7 cell lines is reliant on concentrations of new complexes and time of treatment, while pure cisplatin display only a trend of time dependent inhibitory effect.

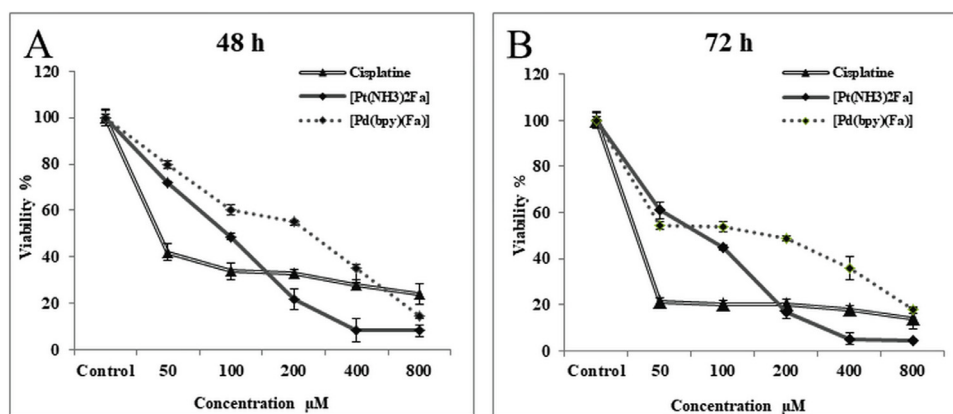


Fig. 4. Cytotoxicity evaluation of cisplatin, cis-[Pt(NH₃)₂FA] and [Pd(bpy)FA] on MCF-7 cell lines after 48 and 72 h of exposure.

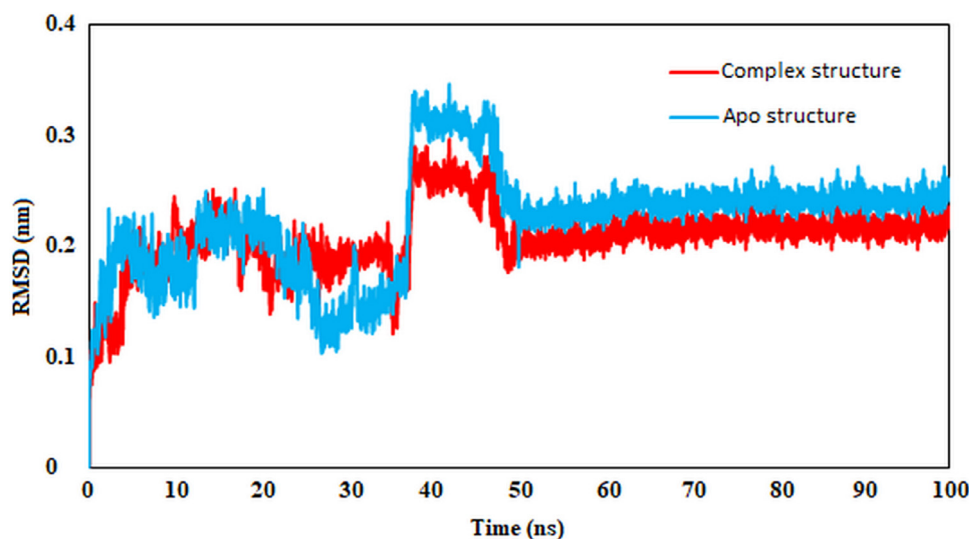


Fig. 5. The root-mean-square deviation (RMSD) (nm) of FR for the backbone atoms in 100 ns MD simulation for two states of apo (blue) and complex (red). (For interpretation of the references to colour in this figure legend, the reader is referred to the web version of this article.)

Table 1
IC₅₀ (μM) values of used compounds in MTT assay.

Compounds	48 h	72 h
Cisplatin	43	33
cis-[Pt(NH ₃) ₂ FA]	96	87
[Pd(bpy)FA]	266	190

So that, the high concentrations of cis-[Pt(NH₃)₂FA] can reduce both cell proliferation and viability to about 5% of the control after 72 h of treatment. In high concentrations, cis-[Pt(NH₃)₂FA] showed better effects as comparison to cisplatin, while [Pd(bpy)FA] had a somewhat weaker effect at all concentrations in contrast with cisplatin.

According to Table 1, the IC₅₀ values of 33, 87 and 190 μM were achieved for cisplatin, cis-[Pt(NH₃)₂FA] and [Pd(bpy)FA] following 72 h of treatment, respectively. All of findings confirm that cis-[Pt(NH₃)₂FA] and [Pd(bpy)FA] could be potential compounds to target FRs on breast cancer cells, and also existence of FA in construction of complexes substantially sustain the release kinetics of cisplatin from the pseudo-carriers.

3.3. Apoptotic gene expression

Cisplatin is able to exert its cytotoxicity to cancer cells via interaction with DNA and proteins which can ultimately result in DNA damage and also cell death [39]. A similar performance is also observed for other planar metal complexes like 2,2'-bipyridine Pd(II), which act as DNA intercalator [38]. Also, several studies have revealed that cisplatin exhibited signs of apoptosis to some extent in leukemic, renal and prostate cells, contrary to earlier reports [38–40]. But, it is clearly confirmed that MCF-7 cell lines are relatively resistant to cisplatin, and by enhancing the sensitivity in MCF-7 using p53 dependent apoptotic pathway or down-regulation of cyclin D1 could increase cisplatin-induced apoptosis [41, 42].

Accordingly, we decided to synthesis two new complexes of Pt and Pd using FA and evaluated the apoptosis ability of them on expression of Bclx, Bak1 and Caspase-3 in MCF-7 cell lines. Because, we hypothesize that on one hand, they are able to specifically target the FR-positive MCF-7 cells; on the other hand, FA may have a noticeable impact on apoptosis of MCF-7 cells. This hypothesis was originated from role of FA in inducing the apoptosis in pre-malignant gastric lesions [43]; Da-Zhong Cao et al. confirmed that treatment by FA affects up-regulation of tumor suppressor gene p53 and down-regulation of apoptosis-associated gene bcl-2.

Therefore investigation on Bcl-2 protein family can provide an initial knowledge about the mitochondria-mediated apoptotic

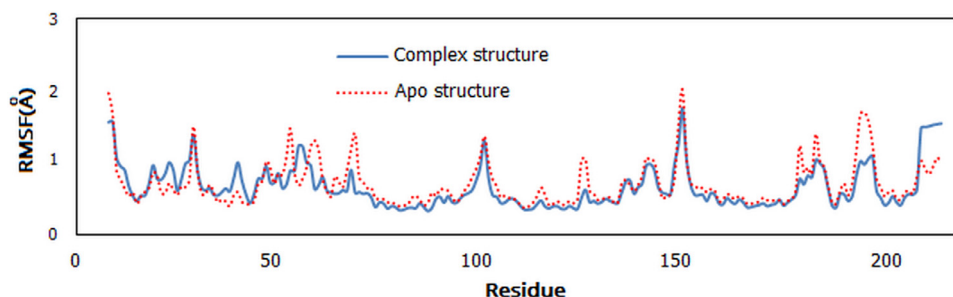


Fig. 6. Atomic positional fluctuations (Å) of C α atoms in the ligand-bound protein (blue line) compared to the ligand-free protein (red dotted line). (For interpretation of the references to colour in this figure legend, the reader is referred to the web version of this article.)

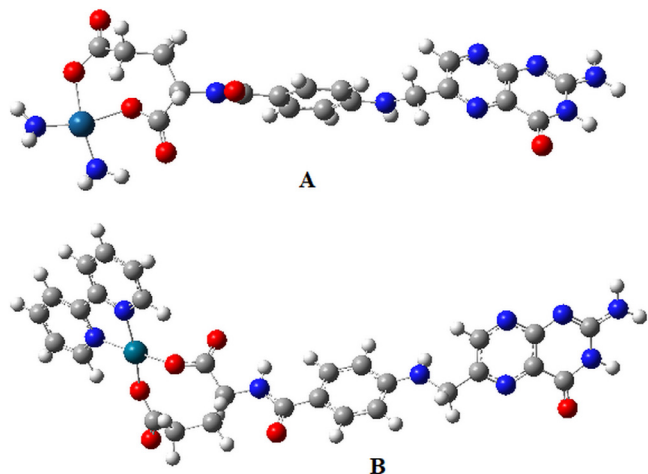


Fig. 7. Optimized geometries of A and B complexes in the gas-phase obtained with the DFT/B3LYP theoretical method.

pathway [44]. Some proteins of this family, including Bcl-2 and Bclx, inhibit apoptosis, while some of them such as Bax and Bak, promote apoptosis. So it seems anti-apoptotic proteins with pro-apoptotic proteins regulate the sensitivity of a cell against apoptosis [45]. For these reasons, we analyzed all complexes' potential capability in expression levels of Bclx and Bak1 in MCF-7 cell lines using real-time PCR. The result demonstrated that the pro-

Table 2

Real-time PCR analysis of mRNA levels of apoptotic genes in MCF-7 cells (Values expressed using RQ which is equal with $2^{-\Delta\Delta CT}$).

	Control	cis-[Pt(NH ₃) ₂ FA]	[Pd(bpy)FA]	Cisplatin
Bclx	1	0.00247	0.0213	1.56
Bak1	1	7.73	0.226	1.59
Caspase-3	1	2.98	0.0486	1.62

tein levels of Bak1 mRNA were significantly upregulated after 24 h of treatment by cis-[Pt(NH₃)₂FA] (Table 2).

As it is evident from Table 2, Bak1/Bclx ratios of synthesized complexes containing FA were increased compared with cisplatin (P-value < 0.05) which confirmed the ability of them in inducing of apoptosis. These ratios for cis-[Pt(NH₃)₂FA] and [Pd(bpy)FA] were 3129 and 10.61, while this ratio for cisplatin was calculated 1.02. Thus the role of FA in inducing apoptosis in the MCF-7 breast cell lines is well characterized.

Unlike the Bcl-2 family of proteins which are the regulators of the intrinsic apoptotic pathway, caspase-3 can active via the intrinsic and extrinsic apoptotic pathways [46]. Thus, the level of caspase-3 activation was determined to further elucidate the apoptosis pathway in MCF-7 cell lines. Results of Table 2 illustrates that cis-[Pt(NH₃)₂FA] increases the levels of caspase-3 associated with apoptosis, therefore it suggests that during treatment with this new complex, the mitochondrial (intrinsic) pathway sensitive to Bak is responsible for caspase-3 activation. While, [Pd(bpy)FA] regulates apoptosis by decreasing the expression of anti-apoptotic

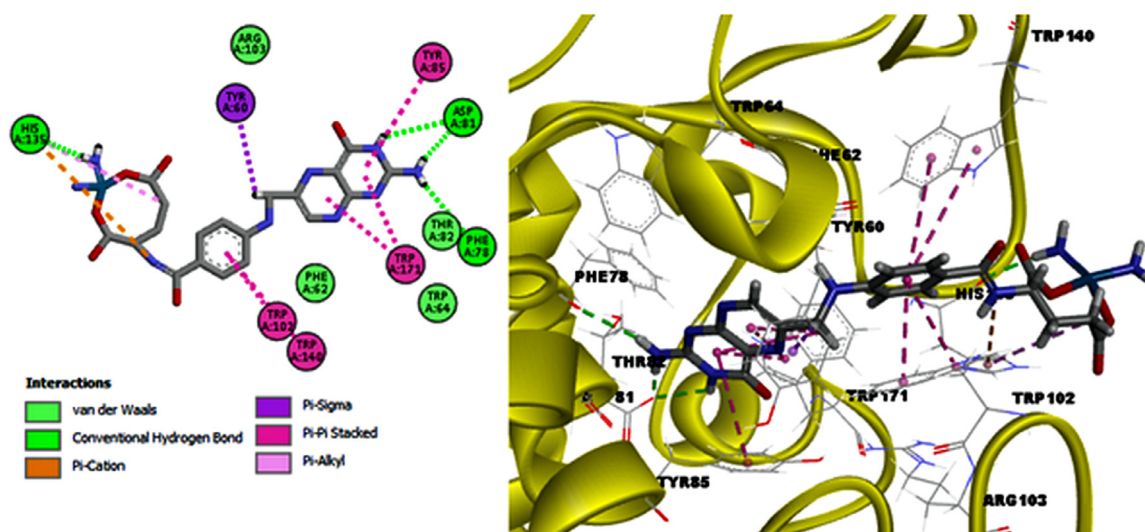


Fig. 8. The 2D and 3D interaction pattern of complex A with FR (pdb ID: 4lh) Hydrogen bond and hydrophobic interactions were shown as green and pink dotted line, respectively. (For interpretation of the references to colour in this figure legend, the reader is referred to the web version of this article.)

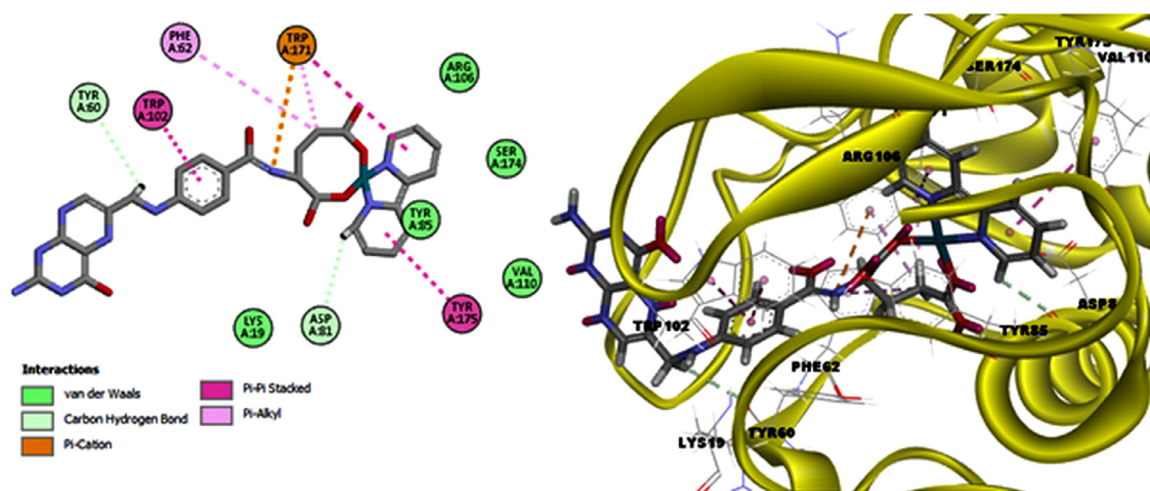


Fig. 9. The 2D and 3D interaction pattern of complex B with FR (pdb ID: 4lrh) Hydrogen bond and hydrophobic interactions were shown as green and pink dotted line, respectively. (For interpretation of the references to colour in this figure legend, the reader is referred to the web version of this article.)

Table 3

ChemScore, binding energy and amino acid residues involved in docking results of complex A and B with FR.

System	Hydrophobic interaction	Hydrogen bond	Van der Waals	binding energy(kcal/mol)	Score
Complex A-FR	TYR60, TYR85,TRP102,TRP140,TRP171	PHE78,ASP81,HIS135	PHE62,TRP64,THR82,ARG103	-38.71	35.72
Complex B-FR	PHE62,TRP102,TRP171,TYR175	TYR60, ASP81	LYS19, TYR85,ARG106,VAL110SER174	-32.23	30.58

Table 4

Hydrogen bond interaction energies and bond length between the complexes A and B with responsive amino acid in molecular docking .

Complex A			Complex B		
Amino acid	Energy(kcal/mol)	Bond length (Å)	Amino acid	Energy(kcal/mol)	Bond length (Å)
ASP81	-2.5	2.64	ASP81	-2.23	2.97
ASP81	-0.31	3.48	TYR60	-2.01	3.019
HIS135	-2.02	3.19			
PHE78	-2.5	2.76			

Bclx levels, but don't have any noticeable effect on expression of caspase-3.

3.4. Molecular dynamic analysis

MD simulation was done in order to provide a more refined and flexible structure systems model for the docking procedure. In this regard, a 100 ns MD simulation was performed on the two-ligand free and ligand-bound systems to obtain multiple conformations of the protein structure. For assessing the conformational stability of the complex and apo enzymes, the trajectory stability and flexibility of the system was analyzed by root-mean-square deviation as functions of time (Fig. 5). The RMSD curve of the simulation confirms that both ligand-bound complex and ligand-free enzymes have reached a stable steady state after 100 ns. Therefore, the trajectories of the MD simulation after equilibrium were reliable for using post-simulation analyses [47-49].

With the aim of determining whether the binding of ligand affects the dynamic behavior of residues, the root mean square fluctuation (RMSF) plot of the backbone C α atoms of the ligand-bound and ligand-free was used to describe flexibility differences among residues. The RMSF of the backbone C α atoms of each residue of apo and in complex with ligand structures were calculated in order to analyze the flexibility of the backbone structure. Higher RMSF value is related to more flexible movement for ligand-free whereas the low one shows less flexibility for ligand-bound forms (Fig. 6).

3.5. Molecular docking analysis

The behavior of small molecules in the binding sites of target proteins can be described by molecular docking, as a complementary method. The method aims to identify correct poses of ligands in the binding site of a protein and to anticipate the affinity between the ligand and the protein. The optimized structures of A and B complexes using DFT calculated are presented in Fig. 7.

Here, complexes A and B were located binding site of the protein by flexible docking using the GOLD program. Table 3 shows the ChemScores fitness value and binding energies of GOLD molecular docking of folate receptor to complexes A and B. The predicted binding energy of complex A-FR interactions (-38.71 kcal/mol and Score=35.72) was higher (more negative) than that complex B-FR interactions (-32.23 kcal/mol and Score=30.58), confirming that complex A could form a more stable complex with FR compared with complex B. In addition, from Table 1 the calculated IC₅₀ values are 87 and 190 μ M for complex A and B in MTT assay following 72 h of treatment, respectively (or 96 and 266 μ M for complex A and B following 48 h). As the inhibition constant can indicate the effectiveness of the ligand in inhibiting biological function of the protein and a smaller value means a greater inhibition potency [50], complex A have a more effective than complex B. This has also been proven by better induction of genes associated with apoptosis. The results of the docking experiments, type of important interaction including hydrogen bond, hydrophobic, and Van der Waals interactions and all near residues for each system docking are shown in Table 3. When a distance between a non-

Table 5

Interaction energy between the complex A and responsive amino acid residues of FR in molecular docking. .

Amino acid residues	Interaction energy kJ mol^{-1}
ASP81	-8.32647
GLN100	-1.20127
HIS135	-21.1998
LYS136	-2.22426
PHE62	-15.6633
PHE78	-1.30742
THR82	-11.9158
TRP64	-1.12735
TRP102	-29.2222
TRP134	-0.3644
TRP138	-1.53823
TRP140	-17.5196
TRP171	-21.6453
TYR60	-17.3048
TYR85	-13.7086

Table 6

Interaction energy between the complex B and responsive amino acid residues of FR in molecular docking. .

Amino acid residues	Interaction energy kJ mol^{-1}
ARG61	-0.48313
ARG103	-5.41557
ARG106	-4.6137
ASP81	-12.1029
LEU84	-4.33754
LEU108	-0.31284
PHE62	-13.8942
PHE78	-0.35241
SER101	-1.49955
SER174	-7.53746
THR82	-7.46916
TRP64	-0.39465
TRP102	-35.6766
TRP140	-20.5384
TRP171	-30.3602
TYR60	-12.0476
TYR85	-25.0334
TYR175	-5.74559
VAL107	-6.38852

hydrogen atom of a protein and ligand is smaller than the sum of their VDW radii plus a threshold of 0.5 Å, a VDW contact can be founded. Nitrogen and oxygen are hydrogen bond acceptors while hydroxyl and amine groups are donor. To form a hydrogen bond, the distance and angle between donor-acceptor should be ≤ 3.5 Å and ≤ 30 , respectively [51]. Hydrogen bonding is the predominant phenomenon in two systems. Hydrogen bond interaction energies and bond length between the two complexes and responsive amino acid in molecular docking are depicted in Table 4. Also, two- and three-dimensional schemes of molecular docking are shown in Figs. 8 and 9. In the end, list of all target residues involved in an interaction with the inspected ligands were display in Tables 5 and 6.

4. Conclusion

Folic acid acts as a bidentate ligand via two monodentate carboxylate groups to form newly complexes with Pt or Pd and control specific endocytosis in breast cancer cells. In line with this claim, MTT assay confirmed that newly synthesized complexes could be potential compounds to target FRs on breast cancer cells and exhibited cytotoxic activity against them. On the other hand, the results of real-time PCR demonstrated that Bak1/Bclx ratios of synthesized complexes containing FA increased compared with cisplatin, and confirmed the ability of them in inducing of apoptosis. Also, the behavior of molecules in the binding sites of target pro-

teins predicted that these complexes could form stable binds with folate receptors and treat the breast cancer cells.

Declaration of Competing Interest

The authors declare that they have no known competing financial interests or personal relationships that could have appeared to influence the work reported in this paper.

CRediT authorship contribution statement

Chenyang He: Writing - review & editing. **Mostafa Heidari Majd:** Supervision, Investigation, Data curation, Writing - original draft. **Fereshteh Shiri:** Conceptualization, Visualization, Software. **Somaye Shahraki:** Methodology, Validation.

Acknowledgments

The authors thank the Deputy of Research and Technology of Zabol University of Medical Sciences, for all support provided.

References

- [1] H. Mansouri-Torshizi, S. Zareian-Jahromi, A. Ghahghaei, S. Shahraki, F. Khosravi, M. Heidari Majd, Palladium(II) complexes of biorelevant ligands. Synthesis, structures, cytotoxicity and rich DNA/HSA interaction studies. *J. Biomol. Struct. Dyn.* 36 (2018) 2787–2806.
- [2] S. Dasari, P.B. Tchounwou, Cisplatin in cancer therapy: molecular mechanisms of action. *Eur. J. Pharmacol.* 740 (2014) 364–378.
- [3] B.J. Pages, D.L. Ang, E.P. Wright, J.R. Aldrich-Wright, Metal complex interactions with DNA. *Dalton Trans.* 44 (2015) 3505–3526.
- [4] A.-M. Florea, D. Büsselberg, Cisplatin as an anti-tumor drug: cellular mechanisms of activity, drug resistance and induced side effects. *Cancers* 3 (2011) 1351–1371.
- [5] S. Shahraki, F. Shiri, Z. Razmara, M.H. Majd, A comparative study of the impact of metal complex size on the in vitro biological behavior of hetero di- and poly-nuclear Mn-Co complexes. *J. Mol. Struct.* 1178 (2019) 617–629.
- [6] A.I. Matesanz, I. Leitao, Souza P., Palladium (II) and platinum (II) bis (thiosemicarbazone) complexes of the 2, 6-diacetylpyridine series with high cytotoxic activity in cisplatin resistant A2780cisR tumor cells and reduced toxicity. *J. Inorg. Biochem.* 125 (2013) 26–31.
- [7] M. Tanaka, H. Kataoka, S. Yano, H. Ohi, K. Kawamoto, T. Shibahara, T. Mizoshita, Y. Mori, S. Tanida, T. Kamiya, Anti-cancer effects of newly developed chemotherapeutic agent, glycoconjugated palladium (II) complex, against cisplatin-resistant gastric cancer cells. *BMC cancer* 13 (2013) 237.
- [8] G. Szóke, A. Takács, Z. Berente, A. Petz, L. Kollár, Synthesis of amino-substituted pyridylglyoxylamides via palladium-catalysed aminocarbonylation. *Tetrahedron* 72 (2016) 3063–3067.
- [9] J.M. Asensio, S. Tricard, Y. Coppel, R. Andrés, B. Chaudret, E. de Jesus, Synthesis of Water-Soluble Palladium Nanoparticles Stabilized by Sulfonated N-Heterocyclic Carbenes. *Chem. Eur. J.* 23 (2017) 13435–13444.
- [10] M.R. Didgikar, S.S. Joshi, S.P. Gupte, M.M. Diwakar, R.M. Deshpande, R.V. Chaudhari, Oxidative carbonylation of amine using water-soluble palladium catalysts in biphasic media. *J Mol Catal A Chem* 334 (2011) 20–28.
- [11] G. Schwartzmann, B. Winograd, H.M. Pinedo, The main steps in the development of anticancer agents. *Radiother. Oncol.* 12 (1988) 301–313.
- [12] A. Sargazi, M. Azhoogh, S. Allahdad, M. Heidari Majd, Evaluation of supramolecule conjugated magnetic nanoparticles as a simultaneous carrier for methotrexate and tamoxifen. *J. Drug Deliv. Sci. Technol.* 47 (2018) 115–122.
- [13] M. Heidari Majd, D. Asgari, J. Barar, H. Valizadeh, V. Kafil, A. Abadpour, E. Mouvivand, J.S. Mojarad, M.R. Rashidi, G. Coukos, Y. Omidi, Tamoxifen loaded folic acid armed PEGylated magnetic nanoparticles for targeted imaging and therapy of cancer. *Colloid. Surf. B: Biointerface.* 106 (2013) 117–125.
- [14] M. Saeidifar, H. Mansouri-Torshizi, A. Divsalar, A.A. Saboury, Novel 2, 2'-bipyridine palladium (II) complexes with glycine derivatives: synthesis, characterization, cytotoxic assays and DNA-binding studies. *J. Iran. Chem. Soc.* 10 (2013) 1001–1011.
- [15] H. Mansouri-Torshizi, M. Eslami-Moghadam, A. Divsalar, A.A. Saboury, DNA-Binding Studies of Some Potential Antitumor 2, 2'-bipyridine Pt (II)/Pd (II) Complexes of piperidinedithiocarbamate. Their synthesis. *Acta Chim. Slov.* (2011) 58.
- [16] A. Sargazi, F. Shiri, S. Keikha, M.H. Majd, Hyaluronan magnetic nanoparticle for mitoxantrone delivery toward CD44-positive cancer cells. *Colloid. Surf. B: Biointerfaces* 171 (2018) 150–158.
- [17] S. Shahraki, M.H. Majd, A. Heydari, Novel tetradentate Schiff base zinc(II) complex as a potential antioxidant and cancer chemotherapeutic agent: Insights from the photophysical and computational approach. *J. Mol. Struct.* 1177 (2019) 536–544.

- [18] A. Sargazi, A. Barani, M. Heidari Majd, Synthesis and Apoptotic Efficacy of Biosynthesized Silver Nanoparticles Using *Acacia luciana* Flower Extract in MCF-7 Breast Cancer Cells: Activation of Bak1 and Bclx for Cancer Therapy, *Bionanoscience* 10 (2020) 683–689.
- [19] J. Barar, V. Kafil, M.H. Majd, A. Barzegari, S. Khani, M. Johari-Ahar, D. Asgari, G. Cokous, Y. Omid, Multifunctional mitoxantrone-conjugated magnetic nanosystem for targeted therapy of folate receptor-overexpressing malignant cells, *J. Nanobiotechnol.* (2015) 13.
- [20] F. Shiri, S. Pirhadi, J.B. Ghasemi, Dynamic structure based pharmacophore modeling of the Acetylcholinesterase reveals several potential inhibitors, *J. Biomolecul. Struct. Dyn.* 37 (2019) 1800–1812.
- [21] C. Chen, J. Ke, X.E. Zhou, W. Yi, J.S. Brunzelle, J. Li, E.L. Yong, H.E. Xu, K. Melcher, Structural basis for molecular recognition of folic acid by folate receptors, *Nature* 500 (2013) 486–489.
- [22] G. Martínez-Rosell, T. Giorgino, G. De Fabritiis, PlayMolecule ProteinPrepare: a web application for protein preparation for molecular dynamics simulations, *J. Chem. Inf. Model.* 57 (2017) 1511–1516.
- [23] E.F. Pettersen, T.D. Goddard, C.C. Huang, G.S. Couch, D.M. Greenblatt, E.C. Meng, T.E. Ferrin, UCSF Chimera—A visualization system for exploratory research and analysis, *J. Comput. Chem.* 25 (2004) 1605–1612.
- [24] A.W.S. Da Silva, W.F. Vranken, ACPYPE-Antechamber python parser interface, *BMC research notes* 5 (2012) 367.
- [25] J.B. Ghasemi, A. Abdolmaleki, F. Shiri, J.B. Ghasemi, Molecular docking challenges and limitations, in: *Pharmaceutical Sciences: Breakthroughs in Research and Practice*, IGI Global, 2017, pp. 770–794.
- [26] A. Abdolmaleki, F. Shiri, J.B. Ghasemi, in: *Computational Multi-Target Drug Design, Multi-Target Drug Design Using Chem-Bioinformatic Approaches*, Springer, 2018, pp. 51–90.
- [27] C.E. Check, T.O. Faust, J.M. Bailey, B.J. Wright, T.M. Gilbert, L.S. Sunderlin, Addition of polarization and diffuse functions to the LANL2DZ basis set for p-block elements, *J. Phys. Chem. A*. 105 (2001) 8111–8116.
- [28] G. Jones, P. Willett, R.C. Glen, A.R. Leach, R. Taylor, Development and validation of a genetic algorithm for flexible docking, *J. Mol. Biol.* 267 (1997) 727–748.
- [29] J. Zhang, S. Rana, R. Srivastava, R. Misra, On the chemical synthesis and drug delivery response of folate receptor-activated, polyethylene glycol-functionalized magnetite nanoparticles, *Acta Biomater* 4 (2008) 40–48.
- [30] Y. He, X. Wang, P. Jin, B. Zhao, X. Fan, Complexation of anthracene with folic acid studied by FTIR and UV spectroscopies, *Spectrochim. Acta A Mol. Biomol. Spectrosc.* 72 (2009) 876–879.
- [31] E. Hamed, M. Attia, K. Bassiouny, Applications, Synthesis, spectroscopic and thermal characterization of copper (II) and iron (III) complexes of folic acid and their absorption efficiency in the blood, *Bioinorg Chem Appl.* (2009) 2009.
- [32] M.A. El-Wahed, M. Refat, S. El-Megharbel, Synthesis, spectroscopic and thermal characterization of some transition metal complexes of folic acid, *Spectrochim. Acta A Mol. Biomol. Spectrosc.* 70 (2008) 916–922.
- [33] Y.L. Lai, C.C. Lin, S.R. Hsu, S.K. Yen, Electrochemical Deposition of Cisplatin on Pure Magnesium, *J. Electrochem. Soc.* 165 (2018) 196–205.
- [34] S.N. Senadheera, T. Zhang, C.E. Groer, M.L. Forrest, Formation of platinum (II) as a six member ring for sustained polymeric delivery, *Eur. J. Med. Chem.* 136 (2017) 452–456.
- [35] A.M. Florea, D. Büsselberg, Cisplatin as an anti-tumor drug: cellular mechanisms of activity, drug resistance and induced side effects, *Cancers* 3 (2011) 1351–1371.
- [36] M. Saeidifar, H. Mirzaei, N.A. Nasab, H. Mansouri-Torshizi, Mononuclear Pd (II) complex as a new therapeutic agent: Synthesis, characterization, biological activity, spectral and DNA binding approaches, *J. Mol. Struct.* 1148 (2017) 339–346.
- [37] Y. Yamada, D. Koori, Y. Oshikawa, M. Koikawa, Stereospecific interaction of optically active sulfur-bridged dinuclear Co(III)–Pt(II) complex with pseudo-enantiomeric Co(III)–M(II) (M: Pd or Pt) complex involving nonequivalent π electronic system, *Inorganica Chim. Acta* 450 (2016) 225–231.
- [38] Z. Sorinezami, H. Mansouri-Torshizi, M. Aminzadeh, A. Ghahghaei, N. Jamgohari, M. Heidari Majd, Synthesis of new ultrasonic-assisted palladium oxide nanoparticles: an in vitro evaluation on cytotoxicity and DNA/BSA binding properties, *J. Biomolecul. Struct. Dyn.* 37 (2019) 4238–4250.
- [39] K.M. Henkels, J.J. Turchi, Cisplatin-induced apoptosis proceeds by caspase-3-dependent and-independent pathways in cisplatin-resistant and-sensitive human ovarian cancer cell lines, *Cancer research* 59 (1999) 3077–3083.
- [40] B.S. Cummings, R.G. Schnellmann, Cisplatin-induced renal cell apoptosis: caspase 3-dependent and-independent pathways, *J. Pharmacol. Exp. Ther.* 302 (2002) 8–17.
- [41] C.W. Yde, O.G. Issinger, Enhancing cisplatin sensitivity in MCF-7 human breast cancer cells by down-regulation of Bcl-2 and cyclin D1, *Int J Oncol* 29 (2006) 1397–1404.
- [42] O. Kutuk, E.D. Arisan, T. Tezil, M.C. Shoshan, H. Basaga, Cisplatin overcomes Bcl-2-mediated resistance to apoptosis via preferential engagement of Bak: critical role of Noxa-mediated lipid peroxidation, *Carcinogenesis* 30 (2009) 1517–1527.
- [43] D.Z. Cao, W.H. Sun, X.L. Ou, Q. Yu, T. Yu, Y.Z. Zhang, Z.Y. Wu, Q.P. Xue, Y.L. Cheng, Effects of folic acid on epithelial apoptosis and expression of Bcl-2 and p53 in premalignant gastric lesions, *World J J* 11 (2005) 1571.
- [44] N. Susnow, L. Zeng, D. Margineantu, D.M. Hockenbery, Bcl-2 family proteins as regulators of oxidative stress, in: *SSemin Cancer Biol*, Elsevier, 2009, pp. 42–49.
- [45] C. Bauer, C. Hees, A. Sterzik, F. Bauernfeind, R. Mak'Anyengo, P. Duedwell, H.-A. Lehr, E. Noessner, R. Wank, A. Trauzold, Proapoptotic and Antiapoptotic Proteins of the Bcl-2 Family Regulate Sensitivity of Pancreatic Cancer Cells Toward Gemcitabine and T-Cell-mediated Cytotoxicity, *J. Immunother.* 38 (2015) 116–126.
- [46] K. Boland, L. Flanagan, J.H. Prehn, Paracrine control of tissue regeneration and cell proliferation by Caspase-3, *Cell Death Dis* 4 (2013) 725.
- [47] K. Kumar, A. Anbarasu, S. Ramaiah, Molecular docking and molecular dynamics studies on β -lactamases and penicillin binding proteins, *Mol Biosyst.* 10 (2014) 891–900.
- [48] E.J. Chaves, I.C.Q. Padilha, D.t.A. Araújo, G.B. Rocha, Determining the Relative Binding Affinity of Ricin Toxin A Inhibitors by Using Molecular Docking and Nonequilibrium Work, *J Chem Inf Model* 58 (2018) 1205–1213.
- [49] N. Sharma, A. Murali, S.K. Singh, R. Giri, Epigallocatechin gallate, an active green tea compound inhibits the Zika virus entry into host cells via binding the envelope protein, *Int. J. Biol. Macromol.* 104 (2017) 1046–1054.
- [50] A. Madeswaran, M. Umamaheswari, K. Asokkumar, T. Sivashanmugam, V. Subhadradevi, P. Jagannath, silico docking studies of phosphodiesterase inhibitory activity of commercially available flavonoids, *Orient. Pharm. Exp. Med.* 12 (2012) 301–306.
- [51] T. Damghani, T. Sedghamiz, S. Sharifi, S. Pirhadi, Critical c-Met-inhibitor interactions resolved from molecular dynamics simulations of different c-Met complexes, *J. Mol. Struct.* 1203 (2020) 127456.